ISSN 0016-7029, Geochemistry International, 2007, Vol. 45, No. 9, pp. 900–917. © Pleiades Publishing, Ltd., 2007.
Original Russian Text © O.A. Limantseva, B.N. Ryzhenko, E.V. Cherkasova, 2007, published in Geokhimiya, 2007, No. 9, pp.981–998.

# Model for the Formation of Fluorine-Bearing Rocks in the Carboniferous Deposits of the Moscow Artesian Basin

**O. A. Limantseva, B. N. Ryzhenko, and E. V. Cherkasova**

*Vernadsky Institute of Geochemistry and Analytical Chemistry, Russian Academy of Sciences, ul. Kosygina 19, Moscow, 119991 Russia*

*e-mail: ryzhenko@geokhi.ru*

Received March 7, 2006; in final form, July 19, 2006

**Abstract**—The paper presents the results of the statistical and thermodynamic analysis of hydrogeochemical information on the genesis of F-bearing waters in the Carboniferous deposits of the Moscow artesian basin. The F concentration is demonstrated to increase with increasing salinity of the aqueous solution. As follows from the analysis of mineral equilibria, the saturation concentrations of the aqueous phase with respect to fluorite in association with calcite and gypsum is less than 2–3 mg of F/l. At the saturation of the aqueous phase with respect to fluorite in association with dolomite, the equilibrium concentration of F increases with increasing Mg concentration and decreasing equilibrium partial $CO_2$ pressure and can reach 8–10 mg of F/l. The main reason for this enrichment of the aqueous phase in F is certain features of mineral equilibria in the system of aqueous solution with Ca and Mg carbonates. An increase in the $Mg^{2+}$ concentration in the aqueous phase decreases the $Ca^{2+}$ concentration in the solubility equilibrium of dolomite, and this, in turn, decreases the $F^-$ concentration in the solubility equilibrium of fluorite.

**DOI:** 10.1134/S0016702907090042

## INTRODUCTION

The territory of Russia includes numerous local geochemical provinces (Moscow, Volga, Cis-Ural, Trans-Ural, Western Siberian, Azov–Kuban', Transbaikalian, and others) in which groundwaters in some aquifers may acquire (under certain naturally occurring or artificially created conditions) high concentrations of F and other chemical elements that complicate the organization of water supply.

Our earlier research [1] has demonstrated that an increase in the concentrations of many elements in groundwaters results from the tendency of the hydrogeochemical system toward the state of chemical equilibrium. Concentrations of F and other elements extending their permissible values is most often a consequence of the tendency of the water–rock system toward chemical equilibrium during the action of natural or artificially induced processes. Below we consider the example of elevated F concentrations in the basin of Moscow oblast.

Our study area was restricted to the southern limb of the Moscow syneclise. The local geology is controlled by the presence of a crystalline basement of Archean–Early Proterozoic age and a sedimentary cover, which consists of Late Proterozoic, Paleozoic, Mesozoic, and Cenozoic rocks. According to hydrogeological zoning, the study area is located at the southern slope of the Moscow artesian basin. The local vertical hydrogeological section is a complicated hydrodynamic system of aquifers that are separated by relatively impermeable strata and rock complexes and may be linked with one another and surface waters [2].

The currently utilized water-producing aquifers and complexes are spatially restricted to fractured carbonate rocks of Late, Middle, and Early Carboniferous age ($C_3$, $C_2$, and $C_1$). The thickness of the freshwater zone is commonly 300–350 m. Over the time of extensive water withdrawal for industrial and domestic purposes, hydrogeological conditions in the Carboniferous aquifers have significantly changed relative to their natural characteristics. The descent of the groundwater table as of 2003 was 20–40 m in the Podolskian–Myachkovskian aquifer, approximately 5 m in the Kashirskian aquifer, and 5–15 m in the Okskian–Protvinskian aquifer.

Over the exploitation time of the Moscow artesian basin, the groundwaters of the Podolskian–Myachkovskian aquifer were determined to contain elevated concentrations of some minor elements, including F and Sr. According to the conclusion drawn by a research team of GEOLINK [3], who conducted hydrogeological field studies of groundwaters in the Moscow area, the possible reasons for an increase in the concentrations of these elements could be (1) the influence of the composition of the host rocks of the Podolskian (which are often enriched in F- and Sr-bearing minerals) and Myachkovskian deposits and (2) the inflow of waters from the Devonian rocks. In other words, although the increase in the F concentration in the Car-

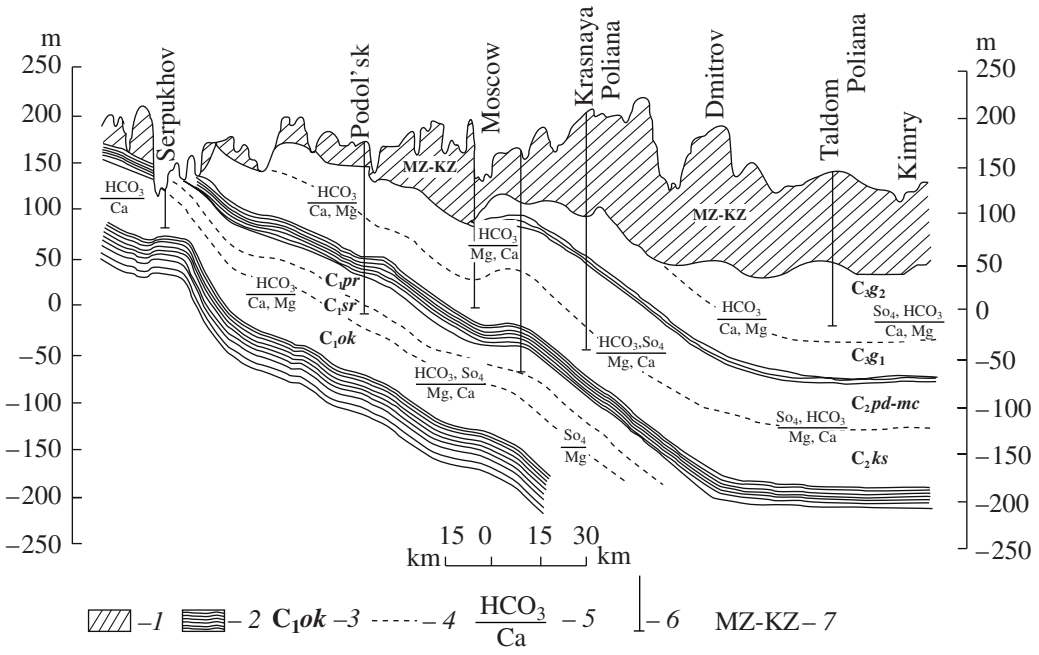


**Fig. 1.** Schematic geological–hydrogeochemical vertical section of the Carboniferous deposits (modified after [2]).
(*1*) Mesozoic and Cenozoic deposits; (*2*) clay deposits; (*3*) aquifer notation; (*4*) boundaries between aquifers; (*5*) hydrogeochemical type of water; (*6*) well; (*7*) Mesozoic and Cenozoic deposits.

boniferous water-producing aquifers of the Moscow artesian basin has been known for a long time, this phenomenon still has not received a convincing explanation. We believe that the inflow and dilution of highly mineralized and fluorian Devonian waters could hardly be regarded as a source of F for the low mineralized Carboniferous waters: the mixing of waters and their dilution to mineralization of hundreds of milligrams per liter should have resulted in a corresponding decrease in the F concentration. In fact, the low mineralized Carboniferous waters bear 5–6 mg/l of F.

It is now pertinent to consider information crucial for the development of a model for the hydrogeochemical processes. The three major zones recognized in the hydrodynamic structure of the basin are as follows: a zone of active regime of groundwaters, a zone of their restricted regime, and a zone of their strongly restricted (stagnant) regime. The aquifers of the Late and Middle Carboniferous deposits and the Okskian–Protvinskian aquifer in the Early Carboniferous deposits belong to the first zone, which is characterized by fresh $HCO_3$–Ca, $HCO_3$–Ca–Mg, and $HCO_3$–$SO_4$–Ca–Mg waters with mineralization no higher than 1 g/l. The zone of restricted water exchange contains brackish $SO_4$–Cl–Ca–Na, $SO_4$–Mg–Ca, $SO_4$–Ca, Cl–$SO_4$–Na, and $SO_4$–Cl–Na waters with mineralization from 1 to 10 g/l (occasionally up to 15 g/l) [4]. This zone includes gypsum-bearing deposits of Early Carboniferous age and an Upper Famennian bed of the latest Devonian. The groundwater temperature changes from 8 to 20°C at depths from 0 to 1000–1200 m. The mineralization of the Carboniferous groundwaters increases with depth and away from watershed areas toward river valleys, i.e., the basin shows a strong correlation between its hydrodynamic and hydrogeochemical zoning (Fig. 1).

The variations in the groundwater types in the course of their flow from the source areas to transit zones are as follows:

$$\frac{HCO_3}{Ca} \rightarrow \frac{HCO_3}{Ca, Mg} \rightarrow \frac{HCO_3}{Mg, Ca} \rightarrow$$

$$\frac{HCO_3, SO_4}{Mg, Ca} \rightarrow \frac{HCO_3, SO_4}{Mg} \rightarrow \frac{SO_4}{Mg} \rightarrow \ldots .$$

It was stated in [2] that the F concentration increases with increasing Mg/Ca ratio (Fig. 2).

## STATISTICAL ANALYSIS

Within the framework of a complex approach to studying particular relations and tendencies and preparatorily to the analysis of the physical chemistry of F enrichment in the Carboniferous groundwaters of the Moscow artesian basin, we quantitatively evaluated links in the hydrochemical system as a part of the water–rock system, based on the correlation analysis and linear regression (in the form of linear trends). No correction (rejection) of the available selection of chemical analyses from [2] was carried out because of the scarcity of the analytical data and the absence of

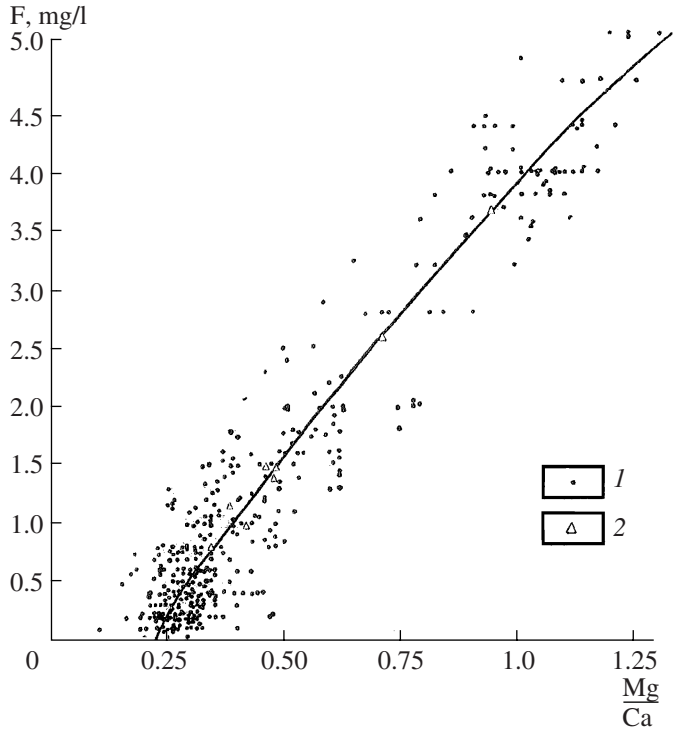


**Fig. 2.** Variations in the F concentration depending on the Mg/Ca ratio in the waters of (*1*) Middle and (*2*) Early Carboniferous (after [2]).

information on the errors in the analyses of the aqueous solutions for chemical elements.

The chemistry–analytical database was subdivided into twelve samplings [first, into three: according to the age of the host rocks ($C_1$, $C_2$, and $C_3$), and then each of them was further subdivided into four groups according to F concentration: F < 0.5 (zone 1), 0.5–1.5 (zone 2), 1.5–3 (zone 3), and >3 mg/l (zone 4), according to [2]] The statistical processing of these data allowed us to reveal various correlations between the mineralization M, the Ca, Mg, $SO_4$, Cl, and F concentrations, and the Mg/Ca ratio (Table 1). The waters of zone 1 of the Late Carboniferous are characterized by the absence of correlations between the concentrations of F and major components; the waters of zone 3 of the Late Carboniferous show a weak correlation between F and Mg (Table 1).

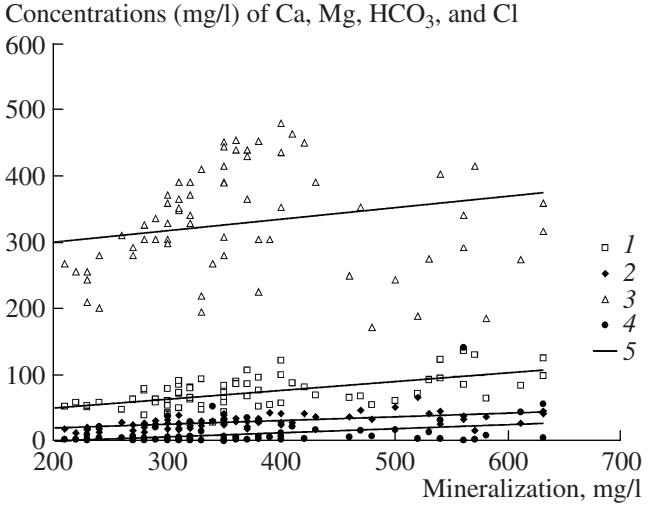


**Fig. 3.** Correlations between the concentration of major components and mineralization: (*1*) Ca, (*2*) Mg, (*3*) $HCO_3$, (*4*) Cl; (*5*) trend.

The data selected for individual beds (from zone 1 through 4) show a weak positive correlation between F concentration and the Mg/Ca ratio (Table 1, Fig. 2). This suggests the operation of certain mechanisms activating links between elements in the databases with F concentrations higher than 1.5 mg/l.

The correlation analysis of the whole database demonstrates that the correlation coefficients are higher than 0.9 (at a significance level $p < 0.05$) between the mineralization and the concentrations of such components as Ca, Mg, $SO_4$, and Cl, and the correlation coefficients between F and Mg and between F and $SO_4$ are equal to 0.5 (Table 1). Of course, the Pearson correlation coefficient is linear and determines only the degree of proportionality of two variables, but nevertheless, this coefficient is a quantitative measure characterizing empirical data, along with their graphical representation.

The analysis of the plots reveals a coupled increase in the concentrations of major ions and mineralization (M to 0.7 g/l) and the further divergence of the slopes of the concentration trajectories (Fig. 3). The tangents of the trends for Ca, Mg, $HCO_3$, and Cl change thereby from 0.1324 to 0.0962, from 0.0575 to 0.0264, from 0.1739 to –0.0418, and from 0.062 to 0.15, respectively, at mineralization of 0–700 and 700–5000 mg/l.

The drastic increase in the concentrations of F and all major components takes place at the intersection of the trajectories for $SO_4$ ($y = 0.6M - 129$ ($R^2 = 0.97$) for $C_3$, $y = 0.3M - 4.6$ ($R^2 = 0.87$) for $C_2$, and $y = 0.7M - 197$ ($R^2 = 0.83$) for $C_1$) and $HCO_3$ ($y = -0.05M + 342$ ($R^2 = 0.38$) for $C_3$, $y = -0.03M + 331$ ($R^2 = 0.39$) for $C_2$, and $y = -0.17M + 407$ ($R^2 = 0.14$) for $C_1$), where $R^2$ is the determination coefficient (Fig. 4). We and the author of [2] identified this inflection point on the trend for the dependence of $HCO_3$ on the mineralization. The inflection suggests a decrease in the equilibrium $CO_2$ partial pressure, i.e., the transformation of the open system carbonate rock–water into a close one [1]. Note that the trends were used solely for the sake of illustration but not for the purpose of prediction or any other purposes.

The graphical dependences (Fig. 4) illustrate the fact that an increase in the mineralization above 0.7 g/l

**Table 1.** Correlation coefficients for the selection of water samples

| Component | Upper Carboniferous, F concentration up to 0.5 mg/l (zone 1) | | | | | | | |
|---|---|---|---|---|---|---|---|---|
| | Ca | Mg | $HCO_3$ | $SO_4$ | Cl | F | M | Mg/Ca |
| Ca | 1 | 0.69 | 0.52 | 0.66 | 0.51 | –0.01 | 0.82 | 0.31 |
| Mg | 0.69 | 1 | 0.60 | 0.53 | 0.60 | –0.48 | 0.86 | 0.89 |
| $HCO_3$ | 0.52 | 0.60 | 1 | –0.19 | –0.21 | –0.39 | 0.26 | 0.57 |
| $SO_4$ | 0.66 | 0.53 | –0.19 | 1 | 0.94 | 0.13 | 0.88 | 0.21 |
| Cl | 0.51 | 0.60 | –0.21 | 0.94 | 1 | –0.15 | 0.87 | 0.40 |
| F | –0.01 | –0.48 | –0.39 | 0.13 | –0.15 | 1 | –0.21 | –0.68 |
| M | 0.82 | 0.86 | 0.26 | 0.88 | 0.87 | –0.21 | 1 | 0.59 |
| Mg/Ca | 0.31 | 0.89 | 0.57 | 0.21 | 0.40 | –0.68 | 0.59 | 1 |
| | Upper Carboniferous, F concentration up to 3.0 mg/l (zone 3) | | | | | | | |
| | Ca | Mg | $HCO_3$ | $SO_4$ | Cl | F | M | Mg/Ca |
| Ca | 1 | 0.79 | –0.86 | 0.99 | 0.97 | 0.19 | 0.99 | –0.40 |
| Mg | 0.79 | 1 | –0.63 | 0.87 | 0.68 | 0.53 | 0.86 | 0.20 |
| $HCO_3$ | –0.86 | –0.63 | 1 | –0.86 | –0.85 | –0.33 | –0.84 | 0.48 |
| $SO_4$ | 0.99 | 0.87 | –0.86 | 1 | 0.94 | 0.31 | 1.00 | –0.27 |
| Cl | 0.97 | 0.68 | –0.85 | 0.94 | 1 | 0.12 | 0.95 | –0.45 |
| F | 0.19 | 0.53 | –0.33 | 0.31 | 0.12 | 1 | 0.27 | 0.43 |
| M | 0.99 | 0.86 | –0.84 | 1.00 | 0.95 | 0.27 | 1 | –0.29 |
| Mg/Ca | –0.40 | 0.20 | 0.48 | –0.27 | –0.45 | 0.43 | –0.29 | 1 |
| | Carboniferous waters (all zones) | | | | | | | |
| | Ca | Mg | $HCO_3$ | $SO_4$ | Cl | F | M | Mg/Ca |
| Ca | 1 | 0.80 | –0.50 | 0.92 | 0.50 | 0.42 | 0.77 | –0.25 |
| Mg | 0.80 | 1 | –0.63 | 0.95 | 0.76 | 0.55 | 0.92 | 0.17 |
| $HCO_3$ | –0.50 | –0.63 | 1 | –0.68 | –0.49 | –0.57 | –0.60 | –0.22 |
| $SO_4$ | 0.92 | 0.95 | –0.68 | 1 | 0.74 | 0.52 | 0.93 | –0.03 |
| Cl | 0.50 | 0.76 | –0.49 | 0.74 | 1 | 0.25 | 0.93 | 0.08 |
| F | 0.42 | 0.55 | –0.57 | 0.52 | 0.25 | 1 | 0.40 | 0.49 |
| M | 0.77 | 0.92 | –0.60 | 0.93 | 0.93 | 0.40 | 1 | 0.02 |
| Mg/Ca | –0.25 | 0.17 | –0.22 | –0.03 | 0.08 | 0.49 | 0.02 | 1 |

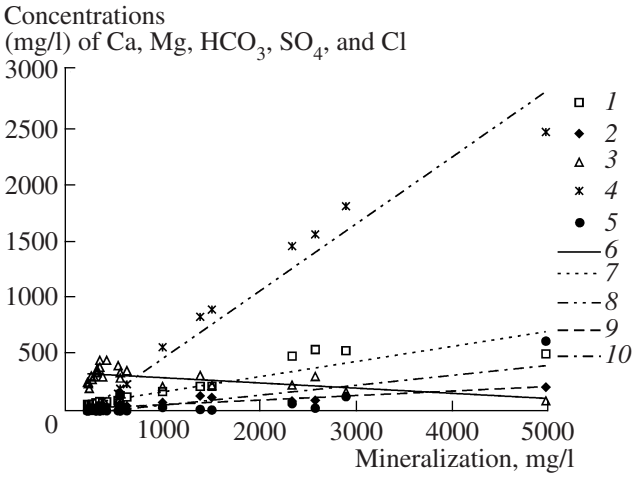


**Fig. 4.** Linear trends for the deposits of the Ca, Mg, $HCO_3$, $SO_4$, and Cl concentrations on the mineralization of waters in Late Carboniferous rocks.

(*1*) Actual Ca concentrations; (*2*) actual Mg concentrations; (*3*) actual $HCO_3$ concentrations; (*4*) actual $SO_4$ concentrations; (*5*) actual Cl concentrations; (*6*) trend for $HCO_3$; (*7*) trend for Ca; (*8*) trend for $SO_4$; (*9*) trend for Mg; (*10*) trend for Cl.

occurs at the cost of sulfate and, to a lesser degree, Ca and Mg.

## PHYSICOCHEMICAL ANALYSIS

Proceeding from the data presented above and chemical analyses compiled from [2], we developed a model for the systematic variations in the chemical composition of water during the filtration of atmospheric precipitate through carbonate deposits. Our method proposed for assaying variations in the chemical composition of groundwaters is underlain by the analysis of mineral equilibria and the physicochemical computer simulations of geochemical processes in water–rock systems. The predominant Carboniferous rocks filling the Moscow syneclise are limestone, dolomite, and, locally, sand and sandstone, and the impermeable strata consist mostly of marl and clay. The major rock-forming minerals of these rocks are calcite, dolomite, quartz, gypsum, siderite, aluminosilicates, anhydrite, micas, and some accompanying minerals containing trace elements (pyrite, fluorite, strontianite, hematite, and others).

The tests of groundwater saturation with respect to the major minerals indicates that water samples borrowed from [2] are oversaturated with respect to calcite, dolomite, fluorite, and strontianite and show systematic variations in the mineral associations along the flow direction of groundwaters. The waters of the source regions are characterized by saturation with respect to calcite alone and simultaneously become oversaturated, first, with respect to calcite and dolomite with depth in the Carboniferous deposits and then with respect to dolomite, fluorite, and strontianite in various combinations (Fig. 5).

Now we can proceed to the analysis of the dependence of the F concentration in the aqueous solution on the concentrations of the major components of groundwaters in a system containing an aqueous solution and the main minerals of carbonate rocks. We use the following notation: $SP_i$ and $K_i$ are the solubility product of a mineral and the ionization constant of complex solute species $i$, and $a_j$ is the activity of aqueous solute species $j$ (in molality units or mg/l). The numerical value of the solubility products of minerals and the constants are listed in Table 2.

For water-hosting rocks containing fluorite, dolomite, gypsum, and calcite, the equilibrium equation of these minerals and the major components of the aque-

**Table 2.** Solubility products of minerals, ionization constants of carbonic acid, and the Henry constant of $CO_2$ at 25°C and 1 bar

| $\log SP_{fl}$ | $\log SP_{cal}$ | $\log SP_{gyp}$ | $\log SP_{dol}$ |
|---|---|---|---|
| $CaF_2 = Ca^{2+} + 2F^-$ | $CaCO_3 = Ca^{2+} + CO_3^{2-}$ | $CaSO_4 \cdot 2H_2O = Ca^{2+} + SO_4^{2-} + 2H_2O$ | $CaMg(CO_3)_2 = Ca^{2+} + Mg^{2+} + 2CO_3^{2-}$ |
| –11.09 | –8.49 | –4.49 | –17.39 |
| $\log K_1$ | $\log K_2$ | $\log K_{Henry}$ | $\log K_w$ |
| $H_2CO_3 = HCO_3^- + H^+$ | $HCO_3 = CO_3^{2-} + H^+$ | $CO_2$ (г) = $CO_2$ (bond) | $H_2O = H^+ + OH^-$ |
| –6.34 | –10.33 | –1.47 | –14.00 |

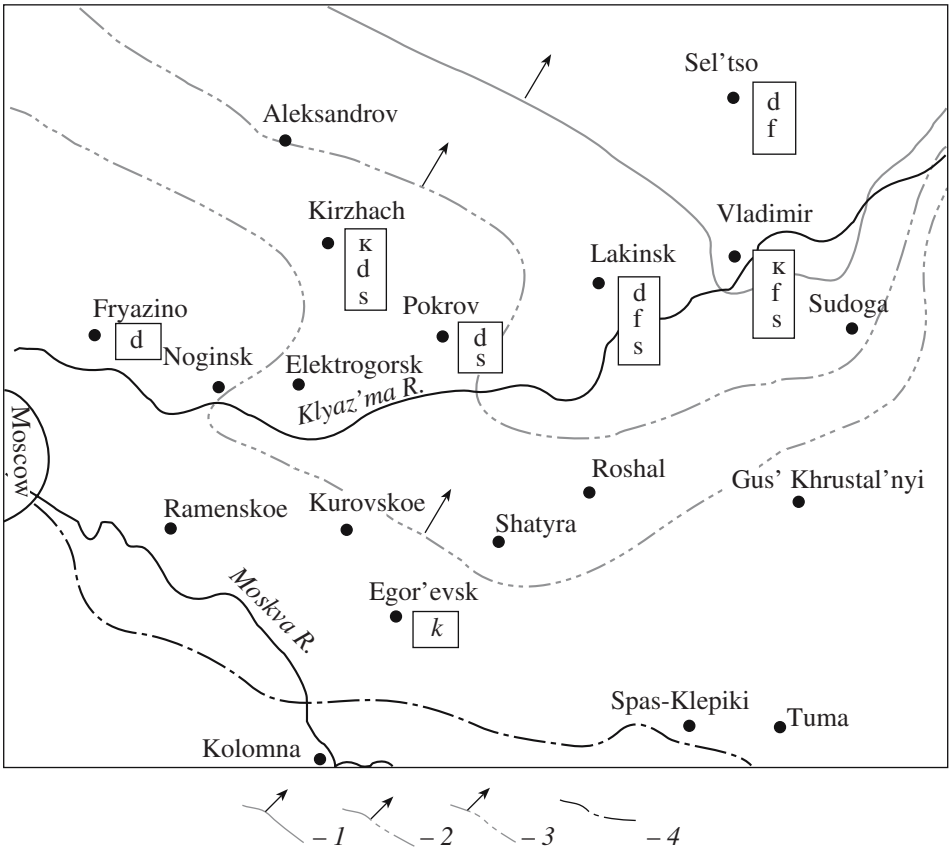


**Fig. 5.** Schematic map for the saturation of waters in Late Carboniferous deposits with respect to various minerals.
F concentrations: (*1*) >3.0 mg/l; (*2*) 1.5–3.0 mg/l; (*3*) 0.5–1.5 mg/l; (*4*) schematized boundary of Late Carboniferous aquifers; *d*—waters saturated with respect to dolomite; *f*—waters saturated with respect to fluorite; *k*—waters saturated with respect to calcite; *s*—waters saturated with respect to strontianite.

ous solution ($Ca^{2+}$, $Mg^{2+}$, $HCO_3^-$, and $SO_4^{2-}$) can be written as

$$a_{Ca^{2+}}(a_{F^-})^2 = SP_{fl},\ a_{Ca^{2+}}a_{CO_3^{2-}} = SP_{cal},$$

$$a_{Ca^{2+}}a_{Mg^{2+}}(a_{CO_3^{2-}})^2 = SP_{dol};\ a_{Ca^{2+}}(a_{SO_4^{2-}})^2 = SP_{gyp},$$

$$a_{CO_3^{2-}} = \frac{K_2 a_{HCO_3^-}}{a_{H^+}} = \frac{K_1 K_2 K_{Henry} P_{CO_2}}{(a_{H^+})^2},$$

$$(a_{F^-})^2 = \frac{SP_{fl}}{a_{Ca^{2+}}} = \frac{a_{SO_4^{2-}} SP_{fl}}{SP_{gyp}}$$

$$= \frac{SP_{fl} K_2^2 a_{HCO_3^-}^2 a_{Mg^{2+}}}{SP_{dol} a_{H^+}^2} = \frac{SP_{fl} SP_{dol}}{(SP_{cal})^2 a_{Mg^{2+}}},$$

$$(a_{F^-})^2 = \frac{a_{CO_3^{2-}} SP_{fl}}{SP_{cal}} = \frac{K_2 a_{HCO_3^-} SP_{fl}}{a_{H^+} SP_{cal}}$$

$$= \frac{K_1 K_2 K_{Henry} P_{CO_2} SP_{fl}}{(a_{H^+})^2 SP_{cal}}.$$

Taking the logarithms of these expressions and substituting the numerical values of *SP* and *K*, we obtain

$$2\log a_{F^-} = \log SP_{fl} - \log a_{Ca^{2+}} = -11.09 - \log a_{Ca^{2+}},$$

$$2\log a_{F^-} = \log SP_{fl} - \log SP_{cal} + \log a_{CO_3^{2-}}$$

$$= -2.60 + \log a_{CO_3^{2-}},$$

$$2\log a_{F^-} = \log SP_{fl} - \log SP_{dol}$$

$$+ 2\log K_2 + 2\log a_{HCO_3^-} + 2\mathrm{pH} + \log a_{Mg^{2+}}$$

$$= -14.36 + 2\log a_{HCO_3^-} + 2\mathrm{pH} + \log a_{Mg^{2+}},$$

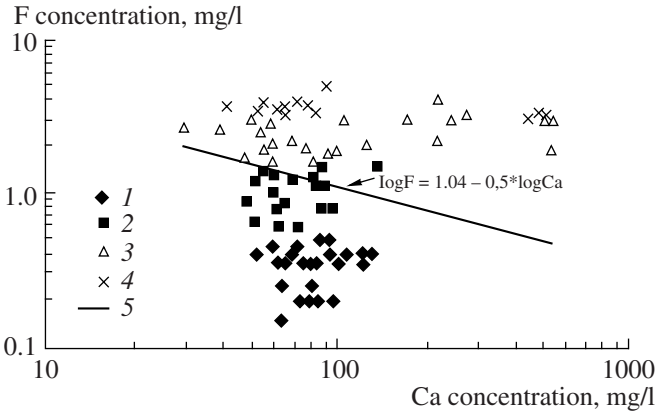


**Fig. 6.** Correlation between the F and Ca concentrations. F concentrations: (*1*) <0.5 mg/l; (*2*) 0.5–1.5 mg/l; (*3*) 1.5–3.0 mg/l; (*4*) >3 mg/l; (*5*) plot for log F = 1.04 – 0.5 × log Ca.

$$2\log a_{F^-} = \log SP_{fl} - \log SP_{gyp} + \log a_{SO_4^{2-}} = -6.60 + \log a_{SO_4^{2-}},$$

$$2\log a_{F^-} = \log SP_{fl} + \log SP_{dol} - 2\log SP_{cal} - \log a_{Mg^{2+}} = -11.50 - \log a_{Mg^{2+}},$$

$$2\log a_{F^-} = \log SP_{fl} - \log SP_{cal} + \log K_2 + \log a_{HCO_3^-} + \mathrm{pH} = -12.93 + \log a_{HCO_3^-} + \mathrm{pH},$$

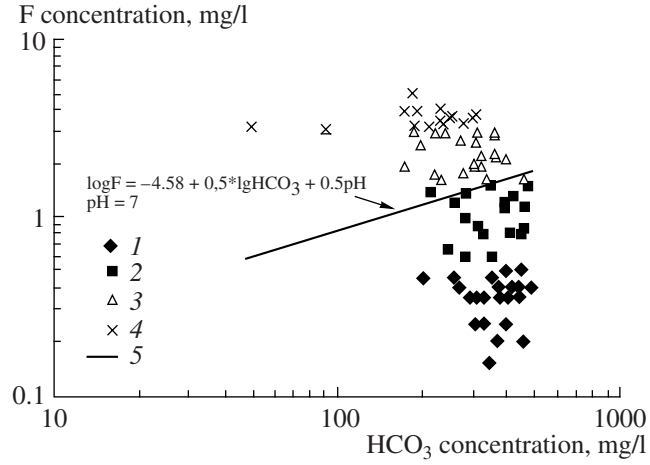


**Fig. 7.** Correlation between the F and hydrocarbonate ion concentrations.
F concentrations: (*1*) <0.5 mg/l; (*2*) 0.5–1.5 mg/l; (*3*) 1.5–3.0 mg/l; (*4*) >3 mg/l; (*5*) plot for log F = –4.58 + 0.5 × log $HCO_3$ + 0.5 pH at pH 7.

$$2\log a_{F^-} = \log SP_{fl} - \log SP_{cal} + \log K_1 + \log K_2 + \log K_{Henry} + \log P_{CO_2} + 2\mathrm{pH} = -20.74 + \log P_{CO_2} + 2\mathrm{pH}.$$

Changing to expressions for concentrations (in mg/l) in place of molality, we then obtain

$$\log a_{F^-} = 1.04 - 0.5\log a_{Ca^{2+}} \quad \text{(aqueous solution + fluorite)}, \tag{1}$$

$$\log a_{F^-} = 0.59 - 0.5\log a_{CO_3^{2-}} \quad \text{(aqueous solution + fluorite + calcite)} \tag{2}$$

$$\log a_{F^-} = -9.24 + \log a_{HCO_3^-} + \mathrm{pH} + 0.5\log a_{Mg^{2+}} \quad \text{(aqueous solution + fluorite + dolomite)}, \tag{3}$$

$$\log a_{F^-} = -1.51 + 0.5\log a_{SO_4^{2-}} \quad \text{(aqueous solution + fluorite + gypsum)}, \tag{4}$$

$$\log a_{F^-} = 0.72 - 0.5\log a_{Mg^{2+}} \quad \text{(aqueous solution + fluorite + calcite + dolomite)}, \tag{5}$$

$$\log a_{F^-} = -4.58 + 0.5\log a_{HCO_3^-} + 0.5\mathrm{pH} \quad \text{(aqueous solution + fluorite + calcite)}, \tag{6}$$

$$\log a_{F^-} = -8.41 + 0.5\log P_{CO_2} + \mathrm{pH} \quad \text{(aqueous solution + fluorite + calcite)}. \tag{7}$$

Equations (1)–(7) explicitly display the dependence of the activity (concentration) of the F ion and the major components of groundwaters contained in carbonate rocks at equilibrium of the aqueous phase with various mineral assemblages (fluorite, fluorite + calcite, fluorite + dolomite, fluorite + gypsum, and fluorite + calcite + dolomite).

Equation (1) describes the dependence between $F^-$ and $Ca^{2+}$ in aqueous solution in equilibrium with fluorite (Fig. 6). Ignoring the difference between the bulk analytical concentration of F (Ca) and the activities of $F^-$ and $Ca^{2+}$, it can be stated that samples from zones 3 and 4 [2] are saturated or oversaturated with respect to fluorite, and samples from zones 1 and 2 are undersaturated with respect to fluorite.

Equations (2), (6), and (7) exhibit the dependences between the activities of $F^-$ and $CO_3^{2-}$ or $HCO_3^-$ or the partial $CO_2$ pressure in the aqueous solution in equilib-

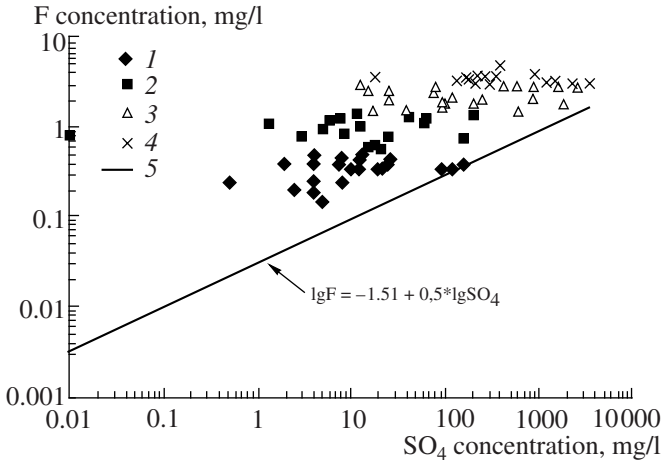


**Fig. 8.** Correlation between the F and sulfate concentrations.

F concentrations: (*1*) <0.5 mg/l; (*2*) 0.5–1.5 mg/l; (*3*) 1.5–3.0 mg/l; (*4*) >3 mg/l; (*5*) plot for log F = –1.51 + 0.5 × log $SO_4$.

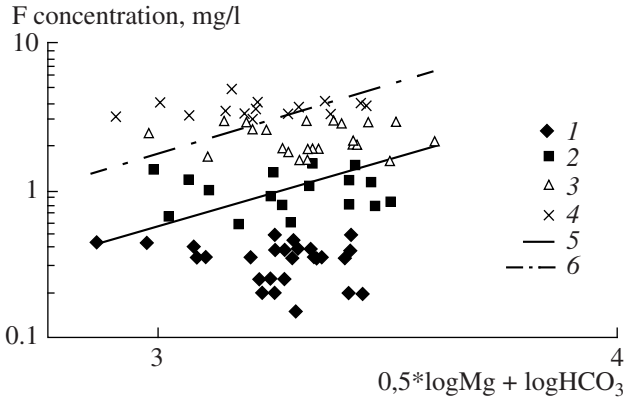


**Fig. 9.** Correlation between the concentrations of F and the sum of Mg and hydrocarbonates at pH 6 and 6.5.

F concentrations: (*1*) <0.5 mg/l; (*2*) 0.5–1.5 mg/l; (*3*) 1.5–3.0 mg/l; (*4*) >3 mg/l; (*5*) plot for log F = –9.24 + 0.5 × log Mg + log $HCO_3$ + pH at pH 6; (*6*) plot for log F = –9.24 + 0.5 × log Mg + log $HCO_3$ + pH at pH 6.5.

rium simultaneously with fluorite and calcite (Fig. 7). Figure 7 shows that the data points of water samples from zones 3 and 4 [2] are saturated or oversaturated with respect to fluorite in association with calcite if the waters have pH 7.

Equation (4) describes the dependence between the $F^-$ and $SO_4^{2-}$ activities in the aqueous solution in equilibrium simultaneously with fluorite and gypsum (Fig. 8). As can be seen from this figure, the data points of water samples from all four zones [2] plot above the saturation line described by Eq. (4), i.e., all samples of the waters would be saturated with respect to fluorite if the latter was in association with gypsum. This conclusion is valid under the assumption that the concentration of $SO_4^{2-} \approx \Sigma SO_4$. Hence, the occurrence of gypsum in the rocks serves as a limiting factor in F enrichment in the groundwaters.

Equation (3) describes the dependence between the activities of $F^-$ and $Mg^{2+}$ in the aqueous solution in equilibrium with fluorite and dolomite (Fig. 9). Equation (5) characterizes the dependence between the activities of $F^-$ and $Mg^{2+}$ in the aqueous solution in equilibrium simultaneously with fluorite, calcite, and dolomite. The arrangement of the data points of the water samples [2] indicates that the dependence between the F and Mg concentrations corresponds to the equilibrium of the aqueous solution with the mineral association fluorite + dolomite [Eq. (3), direct proportionality], whereas the equilibrium of the aqueous solution with the association fluorite + calcite + dolomite [Eq. (5)] is characterized by an inverse proportionality between the F and Mg concentrations.

Now we can conduct a physicochemical simulation of the systematic compositional variations of the aqueous phase during the passage of meteoric waters from the catchment area to the discharge site. The composition of carbonate waters in the Carboniferous deposits of the Moscow syneclise was assumed according to [5]

**Table 3.** Mineral composition (wt %) of rocks assumed in our simulations (numerators) and the reaction progress $\xi$ of the dissolution of this mineral (denominators, $\log\xi$) [1, p. 138]

| Mineral (end member) | Platform carbonate rocks |
|---|---|
| $SiO_2$ | 4.18/–4 |
| $KAlSi_3O_8$ | 0.30/–6 |
| $NaAlSi_3O_8$ | 1.31/–5 |
| $CaAl_2Si_2O_8$ | 0.14/–4 |
| $TiO_2$ | 0.10/–7 |
| $MnO_2$ | 0.06/–7 |
| $K_4MgFeAl_{13}Si_{16}O_{60.5}H_{10}$ | 3.09/–5 |
| $Ca_5(PO_4)_3OH$ | 0.28/–6 |
| $CaMg(CO_3)_2$ | 37.51/–3 |
| $CaCO_3$ | 50.55/–2 |
| $CaSO_4 \cdot 2H_2O$ | 1.99/–1 |
| $CaF_2$ | 0.08/–1 |
| $FeS_2$ | 0.30/–2 |
| NaCl | 0.12/0, –2 |
| C(org) | 0.28/–3 |

**Table 4.** Standard Gibbs free energy values (J/mol) for gases and solid phases used in our simulations [6, 7]

| Solid phases | 25°C, 0.1 MPa |
|---|---|
| $CaCO_3$ (calcite) | –1129258 |
| $MgAl_2Si_2O_{10}H_4$ | –4430954 |
| $Mg_5Al_2Si_3O_{18}H_8$ (clinochlore) | –8263504 |
| AlOOH (diaspore) | –920750 |
| $CaMgC_2O_6$ (dolomite) | –2162010 |
| $CaF_2$ (fluorite) | –1179595 |
| FeOOH (goethite) | –490875 |
| $CaSO_6H_4$ (gypsum) | –1797133 |
| $CaAl_2Si_7O_{18} \cdot 6H_2O$ (heulandite) | –9762573 |
| $Al_2Si_2O_9H_4$ (kaolinite) | –3801800 |
| $MgCO_3$ (magnesite) | –1027799 |
| $SiO_2$ (quartz) | –856479 |
| $SrCO_3$ (strontianite) | –1152566 |
| $Mg_3Si_4O_{12}H_2$ (talc) | –5516826 |

(Table 3). The F concentration in the carbonate rocks was taken up according to [2]. The list of solid phases that can potentially occur in the system includes 80 minerals, some of which were in equilibrium with the aqueous solution (their free energy values are listed in Table 4). The aqueous solution was assumed to contain aqueous solute species, whose free energies are summarized in Table 5.

The equilibrium state of the water–rock system was simulated by the GIBBS program of the HCh software complex [10] with regard for the initial dissolution rates of various minerals [1]. The composition of the modeled aqueous solution and its pH are controlled by the interaction of meteoric water ($H_2O$) and the carbonate rock. The mass ratio of the reacting rock and water (R/W) was varied from $10^{-2}$ to 10 in order to imitate a decrease in the exchange rate.

In as much as we had no reliable information on the $O_2$ and $CO_2$ partial pressures and their variations from the source area to the discharge zone, in our simulations we specified the oxygen partial pressure in such a manner that the Eh of the aqueous phase remained positive within a few hundred millivolts, and the $CO_2$ partial pressure was varied from $10^{-1}$ to $10^{-6}$ bar. Assuming that the exchange rate of the aquifer with the atmosphere gradually decreased as the solution flowed from the source area to the discharge zone [11], we conducted our simulation at decreasing $CO_2$ partial pressure according to the equation $P\ CO_2 = 10^{-1.7 - 0.01 \times i}$, where $i$ is the number of the simulation step, imitating a decrease in the water exchange rate. These variations in the $CO_2$ partial pressure induces a decrease in the $HCO_3$ concentration, as is the case with the natural waters [2], and corresponds to the gradual closure of the system carbonate rock–water with respect to the atmosphere.

The statistical analysis of the variations in the chemical composition of waters in the zones presented in [2] and our data (see above) indicates that the F concentration increases at increasing Mg/Ca ratio. The possible reason for the increase in the Mg/Ca ratio in the aqueous solution could be Mg extraction from aluminosilicate minerals and/or the dissolution of carbonates with Mg/Ca > 1. These possibilities were taken into account in our simulations by means of introducing additional MgO amounts into the composition of the carbonate rock (10–30% excess Mg in the carbonate) or 4–8 mol of additional rapidly extractable Mg per 100 kg of the rock (perhaps, from clay beds).

The results presented in Table 6 and Figs. 10a and 10b demonstrate that the introduction of an additional Mg amount into the rock in the carbonate rock–water system is crucial for the equilibrium mineral assemblage and for the sulfate and fluorine concentrations in the aqueous phase. Without additional Mg (Fig. 10a), the equilibrium mineral assemblage consists of calcite + dolomite + gypsum + fluorite, and the introduction of additional Mg transforms it into dolomite + magnesite + fluorite (Table 6, Fig. 10b). The dependence of the F concentration on the Mg/Ca ratio is shown in Fig. 2 according to the results of the analysis of the samples and, according to our simulation results, in Fig. 11.

**Table 5.** Standard Gibbs free energy values (J/mol) for aqueous solution components used in our simulations [6(ut), 8 (sh), 9 (br)]

| Aqueous solution component | | 25°C, 0.1 MPa | Aqueous solution component | | 25°C, 0.1 MPa |
|---|---|---|---|---|---|
| $H_2O$ | ut | –237141 | $KSO_4^-$ | br | –1031487 |
| $H^+$ | | 0 | $KHSO_4$ | br | –1031939 |
| $OH^-$ | ut | –157262 | $KCO_3^-$ | br | –817180 |
| $H_2$ | sh | 17723 | $KHCO_3$ | br | –867404 |
| $AlO^+$ | sh | –661859 | $Mg^{2+}$ | sh | –453985 |
| AlOOH | sh | –869017 | $MgOH^+$ | br | –624490 |
| $AlO_2^-$ | sh | –831332 | $MgF^+$ | br | –743498 |
| $CO_2$ | sh | –385974 | $MgF_2$ | br | –1034496 |
| $HCO_3^-$ | sh | –586940 | $MgCl^+$ | br | –589042 |
| $CO_3^{2-}$ | sh | –527983 | $MgCl_2$ | br | –720275 |
| $Ca^{2+}$ | sh | –552790 | $MgSO_4$ | br | –1211173 |
| $CaOH^+$ | br | –716616 | $MgHSO_4^+$ | br | –1215049 |
| $CaF^+$ | br | –838422 | $MgCO_3$ | br | –998978 |
| $CaF_2$ | br | –1123940 | $MgHCO_3^+$ | br | –1045891 |
| $CaCl^+$ | br | –68267 | $Na^+$ | sh | –261881 |
| $CaCl_2$ | br | –811717 | NaF | br | –537923 |
| $CaSO_4$ | br | –1309236 | NaCl | br | –388890 |
| $CaHSO_4^+$ | br | –1312941 | $NaSO_4^-$ | br | –100159 |
| $CaCO_3$ | br | –1099724 | $NaCO_3^-$ | br | –797398 |
| $CaHCO_3^+$ | br | –1145666 | $NaHCO_3$ | br | –847280 |
| $Cl^-$ | Sh | –131290 | $SO_4^{2-}$ | sh | –744459 |
| HCl | br | –127240 | $H_2SiO_4^{2-}$ | br | –1176639 |
| $F^-$ | sh | –281751 | $H_3SiO_4^-$ | br | –1253011 |
| HF | br | –299845 | $SiO_2$ | br | –833411 |
| $FeOH^+$ | br | –275536 | $Sr^{2+}$ | sh | –563836 |
| $Fe(OH)_2$ | br | –449352 | $SrF^+$ | br | –846328 |
| $Fe(OH)_3^-$ | br | –383229 | $SrF_2$ | br | –1131561 |
| $FeOH^{2+}$ | br | –241911 | $SrCl^+$ | br | –693699 |
| $Fe(OH)_3$ | br | –660262 | $SrCl_2$ | br | –824018 |
| $Fe(OH)_4^-$ | br | –811817 | $SrSO_4$ | br | –1322850 |
| $K^+$ | sh | –282462 | $SrHSO_4^+$ | br | –1323250 |
| KF | br | –559760 | $SrCO_3$ | br | –1108201 |
| KCl | br | –403763 | $SrHCO_3^+$ | br | –1157797 |

**Table 6.** Influence of an increase in the MgO concentration in the rock on the aqueous phase composition in the system carbonate rock–water at 10°C

| Compositional parameters, phases | Excess MgO = 0 | | | | Excess MgO = 4 ml/100 kg of rock | | | | Excess MgO = 8 ml/100 kg of rock | | | |
|---|---|---|---|---|---|---|---|---|---|---|---|---|
| | R : W | | | | | | | | | | | |
| | 0.01 | 0.1 | 1 | 10 | 0.01 | 0.1 | 1 | 10 | 0.01 | 0.1 | 1 | 10 |
| $\log P_{CO_2}$, gas | –2.20 | –2.32 | –2.45 | –2.57 | –2.20 | –2.32 | –2.45 | –2.57 | –2.20 | –2.32 | –2.45 | –2.57 |
| Aqueous solution composition, mg/l | | | | | | | | | | | | |
| $HCO_3$ | 1.08E + 02 | 2.15E + 02 | 1.20E + 02 | 9.15E + 01 | 1.61E + 02 | 2.15E + 02 | 1.20E + 02 | 9.15E + 01 | 2.51E + 02 | 2.70E + 02 | 1.83E + 02 | 9.99E + 01 |
| Ca | 2.92E + 01 | 7.47E + 01 | 3.42E + 02 | 5.64E + 02 | 2.92E + 01 | 7.47E + 01 | 3.42E + 02 | 5.64E + 02 | 3.50E + 01 | 8.82E + 00 | 1.73E + 01 | 1.17E + 02 |
| Cl | 7.19E – 03 | 6.40E – 02 | 6.82E – 01 | 6.06E + 00 | 1.11E – 05 | 1.47E – 04 | 4.57E – 03 | 5.68E – 02 | 8.64E – 03 | 7.70E – 02 | 8.23E – 01 | 6.10E + 00 |
| F | 8.57E – 01 | 1.44E + 00 | 9.88E – 01 | 9.02E – 01 | 8.57E – 01 | 1.44E + 00 | 9.88E – 01 | 9.02E – 01 | 1.03E + 00 | 4.59E + 00 | 5.27E + 00 | 5.11E + 00 |
| Mg | 3.22E + 00 | 2.37E + 01 | 1.11E + 02 | 1.83E + 02 | 1.39E + 01 | 2.37E + 01 | 1.11E + 02 | 1.83E + 02 | 2.96E + 01 | 8.25E + 01 | 3.84E + 02 | 2.58E + 03 |
| $SO_4$ | 6.84E – 01 | 1.34E + 01 | 2.64E + 02 | 5.29E + 02 | 1.22E + 01 | 1.09E + 02 | 1.17E + 03 | 2.01E + 03 | 1.47E + 01 | 1.31E + 02 | 1.40E + 03 | 1.04E + 04 |
| Sr | 1.94E + 00 | 1.81E + 00 | 1.06E + 01 | 1.86E + 01 | 1.94E + 00 | 1.81E + 00 | 1.06E + 01 | 1.86E + 01 | 1.46E + 00 | 1.17E + 00 | 4.47E + 00 | 3.71E + 01 |
| pH | 7.05 | 7.51 | 7.34 | 7.33 | 7.25 | 7.51 | 7.34 | 7.33 | 7.38 | 7.59 | 7.56 | 7.32 |
| Mineral relative to which the aqueous solution is saturated, % | | | | | | | | | | | | |
| Calcite | 0 | 86.98 | 73.81 | 51.32 | 0 | 4.04 | 8.38 | 1.73 | 0 | 0 | 0 | 0 |
| Mg-aluminosilicate | 0 | 0.01 | 0 | 0 | 0 | 0.01 | 0 | 0 | 0 | 0 | 0 | 0 |
| Clinochlore | 0 | 0 | 0 | 0 | 0 | 0 | 0 | 0 | 0 | 0 | 0.01 | 0.01 |
| Diaspore | 7.43 | 0 | 0 | 0 | 7.34 | 0 | 0 | 0 | 7.28 | 0 | 0 | 0 |
| Dolomite | 0 | 7.81 | 21.66 | 25.26 | 0 | 92.85 | 88.63 | 81.67 | 0 | 98.15 | 88.18 | 87.23 |
| Magnesite | 0 | 0 | 0 | 0 | 0 | 0 | 0 | 0 | 0 | 0 | 9.63 | 10.51 |
| Fluorite | 0 | 2.60 | 2.41 | 1.95 | 0 | 1.55 | 1.59 | 1.38 | 0 | 0.69 | 1.12 | 1.18 |
| Goethite | 92.57 | 0.04 | 0.03 | 0.03 | 92.66 | 0.03 | 0.02 | 0.02 | 92.72 | 0.02 | 0.02 | 0.02 |
| Gypsum | 0 | 0 | 0 | 19.68 | 0 | 0 | 0 | 13.95 | 0 | 0 | 0 | 0 |
| Heulandite | 0 | 0 | 0.02 | 0.01 | 0 | 0 | 0.01 | 0.01 | 0 | 0 | 0 | 0 |
| Quartz | 0 | 0 | 0.01 | 0.04 | 0 | 0 | 0.01 | 0.03 | 0 | 0 | 0.01 | 0.03 |
| Strontianite | 0 | 2.56 | 2.05 | 1.72 | 0 | 1.52 | 1.35 | 1.22 | 0 | 1.13 | 1.04 | 1.03 |

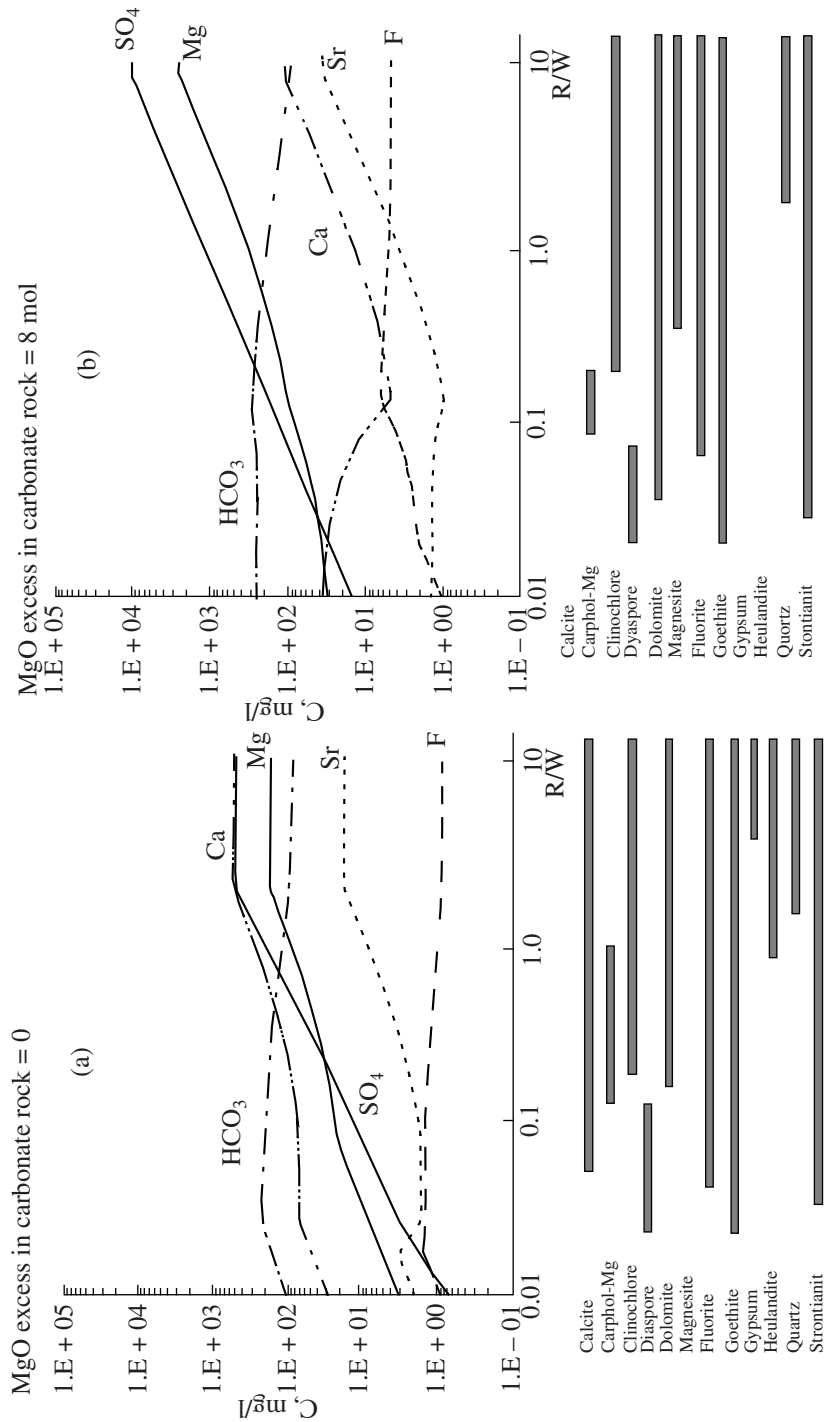


**Fig. 10.** Compositional evolution of the system carbonate rock–water with variations in the rock/water (R/W) ratio. MgO excess in the carbonate rock is (a) 0 and (b) 8 mol.

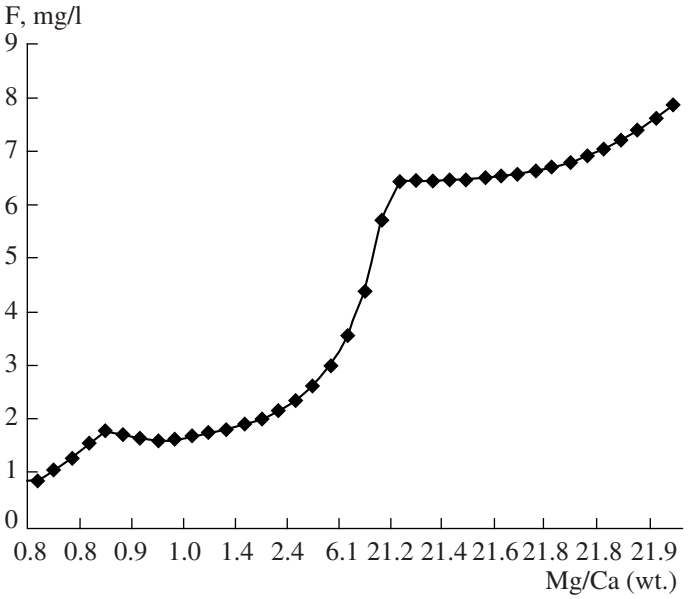


**Fig. 11.** F concentration as a function of the Mg/Ca ratio in the aqueous solution (model).

From the standpoint of chemical equilibria, the mechanism of this effect of Mg on the F concentration in natural aqueous phase in the carbonate rock–water system is as follows. When fluorite dissolves in the aqueous phase after equilibrium was reached, the F concentration is controlled by the $Ca^{2+}$ activity, according to the solubility product for fluorite: $a_{Ca^{2+}}(a_{F^-})^2 = SP_{fl}$ [Eq. (1)]. Hence, the dissolution of minerals supplying Ca for the aqueous phase should decrease the F concentration in the solution in equilibrium with fluorite. Conversely, the Ca concentration during dolomite dissolution depends on the $Mg^{2+}$ activity in the aqueous phase $a_{Ca^{2+}} a_{Mg^{2+}} (a_{CO_3^{2-}})^2 = SP_{dol}$. At other unchanging factors, an increase in the $Mg^{2+}$ concentration in the aqueous solution should result in a decrease in the $Ca^{2+}$ activity and, hence, an increase in the F concentration in the aqueous solution in equilibrium with the fluorite + dolomite association. An additional source of Mg for the aqueous solution can be the dissolution of carbonate with Mg/Ca > 1 and/or an exchange reaction between a Mg aluminosilicate (for example, palygorskite) with components of the aqueous phase.

Another important factor affecting the F concentration in the aqueous solution in the carbonate rock–water system is the equilibrium partial pressure of $CO_2$ (Tables 7, 8; Figs. 12a, 12b, 12c). The character and scale of the effect of equilibrium partial pressure of $CO_2$ on the F concentration in the aqueous solution depend on the mass ratio of the reacting rock and water and on the amount of additional Mg in the system. In all situations, a decrease in the equilibrium partial $CO_2$ pressure in the system carbonate rock–water leads to an increase in the F concentration (Fig. 12a), and the introduction of an additional Mg amount enhances and slightly modifies the character of this dependence (Figs. 12a, 12b). A decrease in the equilibrium partial $CO_2$ pressure results in a decrease in the bicarbonate concentration, an increase in the pH, and an increase in the concentration of sulfate (Tables 7, 8). These relations pervasively occur at a decrease in the partial pressure thanks to the isolation of the system carbonate rock–water at increasing R/W ratio (a decrease in the water exchange rate). Note that the proposed variant of the physicochemical model relatively adequately reflects the actual evolution of the hydrogeochemical composition in the rock strata (Table 9).

$$\frac{HCO_3}{Ca, Mg}\ (R/W \approx 10^{-3}) \longrightarrow \frac{HCO_3}{Mg, Ca}\ (R/W \approx 10^{-2}) \longrightarrow$$

$$\frac{HCO_3, SO_4}{Mg, Ca}\ (R/W \approx 1) \longrightarrow$$

$$\frac{SO_4, HCO_3}{Mg, Ca}\ (R/W \approx 10) \longrightarrow \frac{SO_4}{Mg}\ (R/W \approx 10).$$

**Table 7.** Effect of $CO_2$ partial pressure on the aqueous phase composition in the system carbonate rock–water at 10°C (MgO = = 4 mol)

| Compositional parameters, phases | $\log P_{CO_2} = -1$ | | | | $\log P_{CO_2} = -2$ | | | |
|---|---|---|---|---|---|---|---|---|
| | R : W | | | | | | | |
| | 0.01 | 0.1 | 1 | 10 | 0.01 | 0.1 | 1 | 10 |
| Aqueous solution composition, mg/l | | | | | | | | |
| $HCO_3$ | 4.72E + 02 | 9.83E + 02 | 8.60E + 02 | 8.14E + 02 | 1.73E + 02 | 3.01E + 02 | 2.13E + 02 | 1.91E + 02 |
| Ca | 2.92E + 01 | 1.58E + 02 | 4.40E + 02 | 6.32E + 02 | 2.92E + 01 | 9.00E + 01 | 3.58E + 02 | 5.76E + 02 |
| Cl | 7.19E – 03 | 6.38E – 02 | 6.81E – 01 | 6.06E + 00 | 7.20E – 03 | 6.42E – 02 | 6.86E – 01 | 6.12E + 00 |
| F | 2.15E – 01 | 4.93E – 01 | 9.56E – 01 | 1.30E + 00 | 8.57E – 01 | 1.35E + 00 | 9.76E – 01 | 8.98E – 01 |
| Mg | 1.39E + 01 | 6.61E + 01 | 1.39E + 02 | 2.01E + 02 | 1.39E + 01 | 2.83E + 01 | 1.16E + 02 | 1.86E + 02 |
| $SO_4$ | 9.90E – 01 | 2.17E + 01 | 2.95E + 02 | 5.30E + 02 | 1.22E + 01 | 1.09E + 02 | 1.17E + 03 | 1.99E + 03 |
| Sr | 1.94E + 00 | 4.48E + 00 | 1.33E + 01 | 2.03E + 01 | 1.94E + 00 | 2.18E + 00 | 1.10E + 01 | 1.89E + 01 |
| pH | 6.051 | 6.688 | 6.571 | 6.521 | 7.051 | 7.316 | 7.107 | 7.038 |
| Mineral relative to which the aqueous solution is saturated, % | | | | | | | | |
| Calcite | 0.00 | 0.00 | 7.41 | 1.55 | 0.00 | 1.83 | 8.22 | 1.69 |
| Mg aluminosilicate | 0.00 | 0.00 | 0.00 | 0.00 | 0.00 | 0.00 | 0.00 | 0.00 |
| Clinochlore | 0.00 | 0.00 | 0.00 | 0.00 | 0.00 | 0.00 | 0.00 | 0.00 |
| Diaspore | 7.49 | 0.00 | 0.00 | 0.00 | 7.41 | 0.00 | 0.00 | 0.00 |
| Dolomite | 0.00 | 94.84 | 89.53 | 81.66 | 0.00 | 94.85 | 88.78 | 81.67 |
| Magnesite | 0.00 | 0.00 | 0.00 | 0.00 | 0.00 | 0.00 | 0.00 | 0.00 |
| Fluorite | 0.00 | 2.87 | 1.65 | 1.38 | 0.00 | 1.69 | 1.60 | 1.38 |
| Goethite | 92.51 | 0.05 | 0.02 | 0.02 | 92.59 | 0.03 | 0.02 | 0.02 |
| Gypsum | 0.00 | 0.00 | 0.00 | 14.13 | 0.00 | 0.00 | 0.00 | 13.98 |
| Heulandite | 0.00 | 0.00 | 0.00 | 0.00 | 0.00 | 0.00 | 0.01 | 0.01 |
| Kaolinite | 0.00 | 0.01 | 0.00 | 0.00 | 0.00 | 0.01 | 0.00 | 0.00 |
| Quartz | 0.00 | 0.00 | 0.01 | 0.03 | 0.00 | 0.00 | 0.01 | 0.03 |
| Strontianite | 0.00 | 2.24 | 1.38 | 1.22 | 0.00 | 1.60 | 1.36 | 1.22 |
| Compositional parameters, phases | $\log P_{CO_2} = -3$ | | | | $\log P_{CO_2} = -4$ | | | |
| | R : W | | | | | | | |
| | 0.01 | 0.1 | 1 | 10 | 0.01 | 0.1 | 1 | 10 |
| Aqueous solution composition, mg/l | | | | | | | | |
| $HCO_3$ | 1.27E + 02 | 1.07E + 02 | 6.18E + 01 | 5.39E + 01 | 5.39E + 01 | 3.81E + 01 | 1.91E + 01 | 1.65E + 01 |
| Ca | 2.67E + 01 | 5.38E + 01 | 3.30E + 02 | 5.59E + 02 | 1.52E + 01 | 3.95E + 01 | 3.21E + 02 | 5.53E + 02 |
| Cl | 7.19E – 03 | 6.41E – 02 | 6.82E – 01 | 6.06E + 00 | 7.20E – 03 | 6.42E – 02 | 6.86E – 01 | 6.12E + 00 |
| F | 8.57E – 01 | 1.63E + 00 | 9.98E – 01 | 9.05E – 01 | 8.57E – 01 | 1.83E + 00 | 1.01E + 00 | 9.07E – 01 |
| Mg | 1.24E + 01 | 1.72E + 01 | 1.07E + 02 | 1.82E + 02 | 5.46E + 00 | 1.27E + 01 | 1.05E + 02 | 1.80E + 02 |
| $SO_4$ | 9.09E – 01 | 1.08E + 01 | 2.60E + 02 | 5.29E + 02 | 1.23E + 01 | 1.09E + 02 | 1.17E + 03 | 2.03E + 03 |
| Sr | 7.26E – 01 | 1.31E + 00 | 1.03E + 01 | 1.84E + 01 | 3.59E – 01 | 9.62E – 01 | 1.00E + 01 | 1.83E + 01 |
| pH | 7.996 | 7.911 | 7.622 | 7.543 | 8.633 | 8.471 | 8.127 | 8.045 |
| Mineral relative to which the aqueous solution is saturated, % | | | | | | | | |
| Calcite | 0.00 | 6.60 | 8.49 | 1.74 | 0.00 | 8.12 | 8.59 | 1.77 |
| Mg aluminosilicate | 0.00 | 0.00 | 0.00 | 0.00 | 0.00 | 0.00 | 0.00 | 0.00 |
| Clinochlore | 0.00 | 0.00 | 0.00 | 0.00 | 0.01 | 0.01 | 0.01 | 0.01 |
| Diaspore | 0.01 | 0.00 | 0.00 | 0.00 | 0.00 | 0.00 | 0.00 | 0.00 |
| Dolomite | 91.71 | 90.54 | 88.53 | 81.67 | 97.99 | 89.20 | 88.44 | 81.66 |
| Magnesite | 0.00 | 0.00 | 0.00 | 0.00 | 0.00 | 0.00 | 0.00 | 0.00 |
| Fluorite | 0.00 | 1.38 | 1.59 | 1.38 | 0.00 | 1.26 | 1.58 | 1.38 |
| Goethite | 0.20 | 0.02 | 0.02 | 0.02 | 0.04 | 0.02 | 0.02 | 0.02 |
| Gypsum | 0.00 | 0.00 | 0.00 | 13.93 | 0.00 | 0.00 | 0.00 | 13.91 |
| Heulandite | 0.00 | 0.00 | 0.01 | 0.01 | 0.00 | 0.00 | 0.00 | 0.00 |
| Kaolinite | 0.00 | 0.00 | 0.00 | 0.00 | 0.00 | 0.00 | 0.00 | 0.00 |
| Quartz | 0.00 | 0.00 | 0.01 | 0.03 | 0.00 | 0.00 | 0.01 | 0.03 |
| Strontianite | 8.07 | 1.44 | 1.35 | 1.22 | 1.96 | 1.39 | 1.35 | 1.22 |

**Table 8.** Effect of $CO_2$ partial pressure on the aqueous phase composition in the system carbonate rock–water at 10°C (MgO = 8 mol)

| Compositional parameters, phases | $\log P_{CO_2} = -1$ | | | | $\log P_{CO_2} = -2$ | | | |
|---|---|---|---|---|---|---|---|---|
| | R : W | | | | | | | |
| | 0.01 | 0.1 | 1 | 10 | 0.01 | 0.1 | 1 | 10 |
| Aqueous solution composition, mg/l | | | | | | | | |
| $HCO_3$ | 5.26E + 02 | 1.00E + 03 | 1.18E + 03 | 8.80E + 02 | 2.28E + 02 | 3.40E + 02 | 3.42E + 02 | 2.34E + 02 |
| Ca | 2.92E + 01 | 8.23E + 01 | 2.16E + 01 | 1.23E + 02 | 2.92E + 01 | 2.13E + 01 | 1.59E + 01 | 1.18E + 02 |
| Cl | 7.20E – 03 | 6.42E – 02 | 6.86E – 01 | 6.10E + 00 | 7.20E – 03 | 6.42E – 02 | 6.86E – 01 | 6.10E + 00 |
| F | 8.87E – 01 | 1.90E + 00 | 6.44E + 00 | 7.82E + 00 | 8.57E – 01 | 2.94E + 00 | 5.30E + 00 | 5.12E + 00 |
| Mg | 2.47E + 01 | 1.16E + 02 | 4.63E + 02 | 2.68E + 03 | 2.46E + 01 | 7.77E + 01 | 3.51E + 02 | 2.60E + 03 |
| $SO_4$ | 1.23E + 01 | 1.09E + 02 | 1.17E + 03 | 1.04E + 04 | 1.23E + 01 | 1.09E + 02 | 1.17E + 03 | 1.04E + 04 |
| Sr | 1.94E + 00 | 4.27E + 00 | 5.30E + 00 | 3.86E + 01 | 1.94E + 00 | 1.75E + 00 | 4.01E + 00 | 3.74E + 01 |
| pH | 6.19 | 6.70 | 6.77 | 6.53 | 7.18 | 7.36 | 7.323 | 7.03 |
| Mineral relative to which the aqueous solution is saturated, % | | | | | | | | |
| Calcite | 0 | 0 | 0 | 0 | 0 | 0 | 0 | 0 |
| Mg aluminosilicate | 0 | 0 | 0 | 0 | 0 | 0 | 0 | 0 |
| Clinochlore | 0 | 0 | 0 | 0 | 0 | 0 | 0.01 | 0.01 |
| Diaspore | 7.49 | 0 | 0 | 0 | 7.36 | 0 | 0 | 0 |
| Dolomite | 0 | 97.17 | 91.07 | 87.41 | 0 | 97.96 | 88.64 | 87.23 |
| Magnesite | 0 | 0 | 6.67 | 10.33 | 0 | 0 | 9.15 | 10.51 |
| Fluorite | 0 | 1.5 | 1.16 | 1.18 | 0 | 0.88 | 1.13 | 1.18 |
| Goethite | 92.51 | 0.03 | 0.02 | 0.02 | 92.64 | 0.02 | 0.02 | 0.02 |
| Gypsum | 0 | 0 | 0 | 0 | 0 | 0 | 0 | 0 |
| Heulandite | 0 | 0 | 0 | 0 | 0 | 0 | 0 | 0 |
| Kaolinite | 0 | 0 | 0 | 0 | 0 | 0 | 0 | 0 |
| Quartz | 0 | 0 | 0.01 | 0.03 | 0 | 0 | 0.01 | 0.03 |
| Strontianite | 0 | 1.3 | 1.07 | 1.03 | 0 | 1.14 | 1.05 | 1.03 |
| Compositional parameters, phases | $\log P_{CO_2} = -3$ | | | | $\log P_{CO_2} = -4$ | | | |
| | R : W | | | | | | | |
| | 0.01 | 0.1 | 1 | 10 | 0.01 | 0.1 | 1 | 10 |
| Aqueous solution composition, mg/l | | | | | | | | |
| $HCO_3$ | 1.28E + 02 | 1.64E + 02 | 1.02E + 02 | 5.89E + 01 | 5.58E + 01 | 6.04E + 01 | 3.24E + 01 | 1.81E + 01 |
| Ca | 1.81E + 01 | 2.91E + 00 | 1.40E + 01 | 1.16E + 02 | 6.69E + 00 | 2.00E + 00 | 1.33E + 01 | 1.16E + 02 |
| Cl | 7.18E – 03 | 6.38E – 02 | 6.74E – 01 | 5.69E + 00 | 7.20E – 03 | 6.42E – 02 | 6.86E – 01 | 6.10E + 00 |
| F | 8.57E – 01 | 7.56E + 00 | 5.43E + 00 | 5.11E + 00 | 8.57E – 01 | 7.64E + 00 | 5.48E + 00 | 5.11E + 00 |
| Mg | 1.79E + 01 | 6.35E + 01 | 3.11E + 02 | 2.57E + 03 | 1.10E + 01 | 4.39E + 01 | 2.98E + 02 | 2.56E + 03 |
| $SO_4$ | 9.59E – 01 | 1.49E + 01 | 3.02E + 02 | 4.54E + 03 | 1.23E + 01 | 1.09E + 02 | 1.17E + 03 | 1.04E + 04 |
| Sr | 7.16E – 01 | 5.79E – 01 | 3.56E + 00 | 3.70E + 01 | 3.37E – 01 | 3.98E – 01 | 3.41E + 00 | 3.68E + 01 |
| pH | 8.00 | 8.10 | 7.85 | 7.54 | 8.65 | 8.67 | 8.36 | 8.04 |
| Mineral relative to which the aqueous solution is saturated, % | | | | | | | | |
| Calcite | 0 | 0 | 0 | 0 | 0 | 0 | 0 | 0 |
| Mg aluminosilicate | 0 | 0 | 0 | 0 | 0 | 0 | 0.04 | 0.04 |
| Clinochlore | 0 | 0.01 | 0.01 | 0.01 | 0.01 | 0.01 | 0.01 | 0.01 |
| Diaspore | 0 | 0 | 0 | 0 | 0 | 0 | 0 | 0 |
| Dolomite | 98.05 | 98.82 | 87.81 | 87.17 | 98.73 | 93.7 | 87.58 | 87.22 |
| Magnesite | 0 | 0.01 | 10.01 | 10.57 | 0 | 5.19 | 10.22 | 10.51 |
| Fluorite | 0 | 0.01 | 1.12 | 1.18 | 0 | 0 | 1.11 | 1.18 |
| Goethite | 0.05 | 0.02 | 0.02 | 0.02 | 0.02 | 0.02 | 0.02 | 0.02 |
| Gypsum | 0 | 0 | 0 | 0 | 0 | 0 | 0 | 0 |
| Heulandite | 0 | 0 | 0 | 0 | 0 | 0 | 0 | 0 |
| Kaolinite | 0 | 0 | 0 | 0 | 0 | 0 | 0 | 0 |
| Quartz | 0 | 0 | 0.01 | 0.03 | 0 | 0 | 0 | 0 |
| Strontianite | 1.9 | 1.13 | 1.04 | 1.03 | 1.24 | 1.08 | 1.04 | 1.03 |

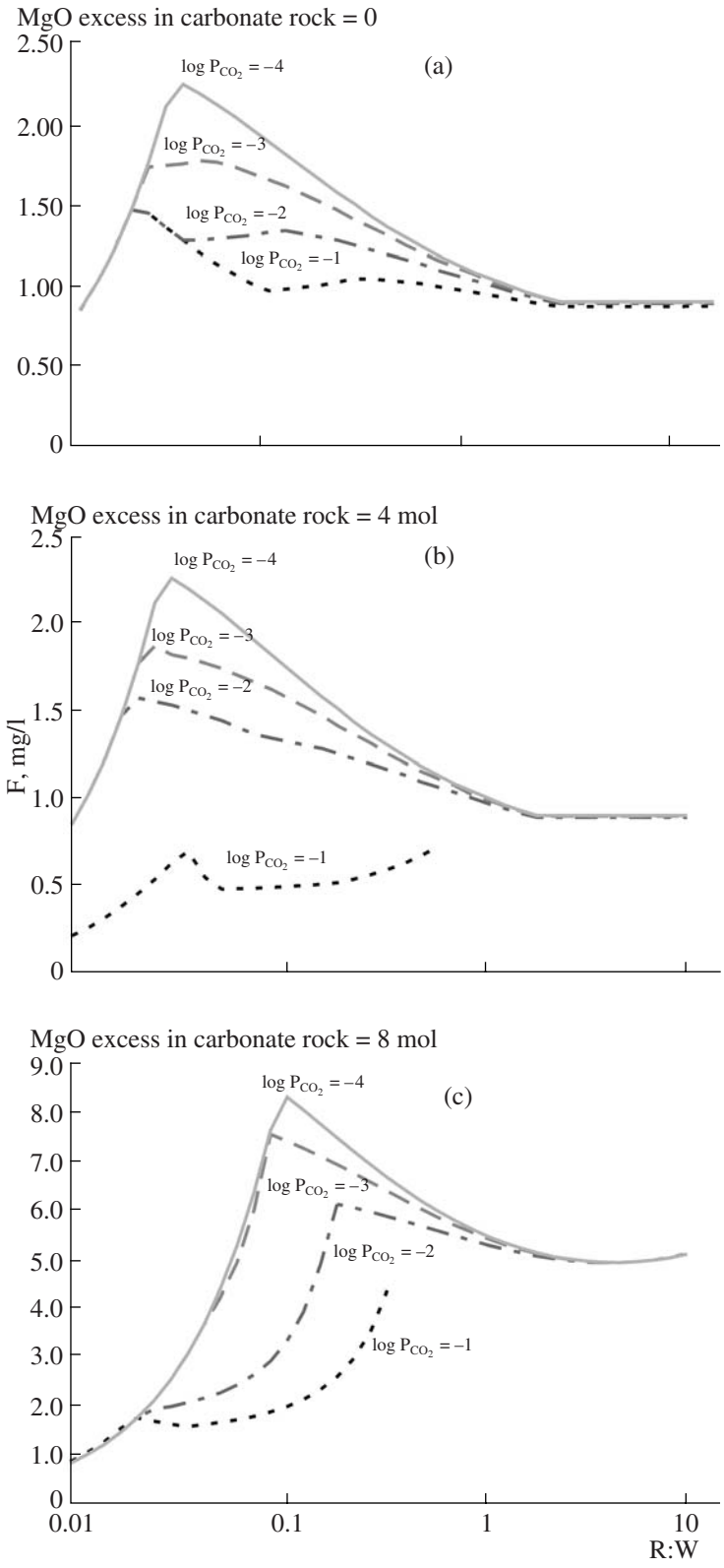


**Fig. 12.** Variations in the F concentration in the aqueous solution of the system carbonate rock–water with variations in the rock/water (R/W) ratio at various equilibrium $CO_2$ partial pressures.

**Table 9.** Comparison of modeled and measured characteristics

| | Hydrogeochemical type of water | | | |
|---|---|---|---|---|
| Model | $\frac{HCO_3}{CaMg}$ | $\frac{HCO_3}{CaMg}$ $\frac{HCO_3SO_4}{CaMg}$ | $\frac{HCO_3SO_4}{CaMg}$ $\frac{SO_4HCO_3}{CaMg}$ $\frac{SO_4}{CaMg}$ $\frac{SO_4}{MgCg}$ $\frac{SO_4}{Mg}$ | $\frac{SO_4}{Mg}$ |
| Fluorine concentration, mg/l | <0.5 | 0.5–1.5 | 1.5–3.0 | >3.0 |
| Measurements | $\frac{HCO_3}{CaMg}$ | $\frac{HCO_3}{CaMg}$ $\frac{HCO_3SO_4}{CaMg}$ $\frac{HCO_3}{MgCg}$ | $\frac{HCO_3SO_4}{CaMg}$ $\frac{HCO_3}{CaMg}$ $\frac{HCO_3SO_4}{MgCg}$ $\frac{HCO_3}{MgCg}$ $\frac{SO_4}{CaMg}$ | $\frac{SO_4}{Mg}$ $\frac{SO_4}{CaMg}$ $\frac{HCO_3SO_4}{MgCg}$ |

## CONCLUSIONS

1. The analysis of general hydrogeochemical conditions revealed the presence of a sharp boundary of the predominance of sulfate ions over hydrocarbonate ions in the Carboniferous waters starting at mineralization of 0.7 g/l. The F concentration thereby practically does not change at mineralization >1 g/l, and the correlation between the F concentration and mineralization weakens from 0.5 to 0.3. In other words, salinity does not affect the F concentration in the water.

2. The analysis of selected correlation coefficients revealed strengthening in the correlations between the F concentration and the Mg concentration and Mg/Ca ratio in the aqueous solution (at an increase in their values). This tendency can be traced in individual rock strata, but the correlation weakens for the whole database at increasing mineralization. This highlights the "hampering" effect of mineralization (more specifically, sulfates, as the predominant minerals, at values higher than 0.7 g/l) on F enrichment and simultaneously emphasizes a positive correlation between F and certain components of the groundwaters.

3. The analysis of data on the composition of waters in the carbonate deposits [2] allowed us to recognize the following hydrogeochemical types: zone 1, F < 0.5 mg/l, $\frac{HCO_3}{Ca, Mg}$; zone 2, F 0.5–1.5 mg/l, $\frac{HCO_3}{Ca, Mg}$; zone 3, F 1.5–3.0 mg/l, $\frac{HCO_3}{Ca, Mg}$, $\frac{HCO_3, SO_4}{Ca, Mg}$; zone 4 F > 3.0 mg/l, $\frac{SO_4}{Ca, Mg}$, $\frac{HCO_3}{Mg, Ca}$, $\frac{HCO_3, SO_4}{Mg, Ca}$. As can be seen, an increase in the mineralization is coupled with greater diversity of the hydrogeochemical types of the waters, and this testifies that the influence of some factors on the composition of the waters gives way to the influence of other factors, i.e., the geochemical parameters (chemical composition and lithology of the rocks) start to dominate over hydrogeochemical parameters (water exchange rate).

4. The successive saturation of the Carboniferous waters in carbonates (calcite ⟶ dolomite ⟶ fluorite and strontianite) along the flow course of the groundwaters from the source area to the discharge zone indicates that the hydrogeochemical processes of the system are gradually modified, and this results in F enrichment.

5. It follows from the analysis of mineral equilibria in the system carbonate rock–water that the saturation concentration of the aqueous phase with respect to fluorite in association with calcite or gypsum is <2–3 mg F/l. As the aqueous phase becomes saturated with respect to fluorite in association with dolomite, the level of equilibrium F concentration increases at increasing Mg concentration and decreasing equilibrium partial pressure of $CO_2$ and can reach 8–10 mg/l F. The main reason for this enrichment of the aqueous phase in F is the character of mineral equilibria in the system aqueous solution–carbonates. An increase in the $Mg^{2+}$ concentration in the aqueous phase decreases the $Ca^{2+}$ concentration in the solubility equilibrium of dolomite, which in turn, increases the $F^-$ concentration in the solubility equilibrium of fluorite. Another reason for the increase in the F concentration in the aqueous phase of the system carbonate rock–water is a decrease in the equilibrium partial $CO_2$ pressure, which leads to an increase in the pH and the concentrations of sulfates in the aqueous phase.

6. Our results demonstrate that the approach applied to studying the genesis of the chemical composition of groundwaters with the use of thermodynamic simulations is also applicable for the solution of problems related to the identifications and timeless prediction of the enrichment of trace elements, including F, in groundwaters.

## ACKNOWLEDGMENTS

The authors thank S.R. Krainov, I.S. Pashkovskii, and the research team of GEOLINK for provided materials and the discussion of our results. This study was supported by the Russian Foundation for Basic Research, project nos. 04-05-64673 and 06-05-08021.

## REFERENCES

1. S. R. Krainov, B. N. Ryzhenko, and V. M. Shvets, *Geochemistry of Groundwaters. Theoretical, Applied, and Ecological Aspects* (Nauka, Moscow, 2004) [in Russian].
2. O. I. Voroshilov, *Fluorine Geochemistry in the Carboniferous Waters of the Moscow Artesian Basin* (Nedra, Moscow, 1972) [in Russian].
3. GEOLINK. Personal Communication.
4. *Hydrogeology of Europe. Vol. 1. General Characteristics of Underground Waters*, Ed. by N. A. Marinov and N. I. Tolstikhin (Nedra, Moscow, 1989) [in Russian].
5. O. M. Rosen, A. A. Abbyasov, A. A. Migdisov, and A. A. Yaroshevskii, " MINLITH—A Program to Calculate the Normative Mineralogy of Sedimentary Rocks: the Reliability of Results Obtained for Deposits of Old Platforms," Geokhimiya, No. 4, 431–444 (2000) [Geochem. Int. **38**, 388–400 (2000)].
6. M. V. Borisov and Yu. V. Shvarov, *Thermodynamics of Geochemical Processes* (Mosk. Gos. Univ., Moscow, 1992) [in Russian].
7. T. Holland and R. Powell, "An Internally Consistent Thermodynamic Dataset for Phases of Petrological Interest," J. Metamorph. Petrol. **16**, 309–343 (1998).
8. E. L. Shock, D. C. Sassani, M. Willis, and D. A. Sverjensky, "Inorganic Species in Geological Fluids. Correlation among Standard Molal Thermodynamic Properties of Aqueous Ions and Complexes," Geochim. Cosmochim. Acta **61** (5), 907–950 (1997).
9. B. N. Ryzhenko, S. R. Krainov, and Yu. V. Shvarov, "Physicochemical Factors Forming the Composition of Natural Waters: Verification of the Rock–Water Model," Geokhimiya, No. 6, 630–640 (2003) [Geochem. Int. **41**, 565–575 (2003)].
10. Yu. V. Shvarov, "Algorithmization of the Numeric Equilibrium Modeling of Dynamic Geochemical Processes," Geokhimiya, No. 6, 646–652 (1999) [Geochem. Int. **37**, 571–576 (1999)].
11. S. L. Shvartsev, *Hydrochemistry of the Hypergene Zone* (Nedra, Moscow, 1998) [in Russian].